CRITICAL REVIEWS IN BIOTECHNOLOGY AND LIFE SCIENCES
Vol: 2 -- Issue: 2 2025
Website: https://crbls.com
Email: editor@crbls.com
ISSN Print: (3080-7093) ISSN Online: (3080-7107)

IMAGING-PATHOLOGIC CORRELATION IN PREOPERATIVE TUMOR STAGING: A RADIOLOGIC PERSPECTIVE

Zia Ur Rehman [1*], Dr. Areeba Khan[2]

[1,] Institute of Biological Sciences, Gomal University, Dera Ismail Khan 29050, Khyber Pakhtunkhwa, Pakistan

[2] Department of Radiology, Shifa International Hospital / Shifa Tameer-e-Millat University, Islamabad, Pakistan

*Corresponding Author E-mail: k.zia59@yahoo.com

Abstract

Staging a tumor properly before the surgery is crucial to make a decision on ways to treat the tumor, predict the effectiveness of treatment and make the optimal surgical plan. This study has cautiously evaluated the relationship of multimodal radiologic imaging such as contrast enhanced computer tomography, high resolution magnetic resonance imaging, and targeted ultrasonography, and subsequent histopathological outcome of a heterogeneous group of solid tumors. The results showed that MRI had the best overall sensitivity (up to 92%) in assessing the extent of local tumors, particularly when it involved soft-tissue dominant cancers, but that CT had a better specificity (87) in detecting regional nodal involvement. Ultrasonography displayed moderate accuracy but presented important real time characterisation of the superficial lesions. Pathologic analysis revealed that in 18% of cases, imaging had slightly underestimated microscopic tumor infiltration, and in 9% cases, excessive extraregional dissemination, which showed the need to integrate morphologic and functional imaging biomarkers and histologic validation. The general consensus of the imaging and pathological staging was over 80%. Tumors with clear margins and minimal stromal invasion were observed to be the best agreement. These results highlight the crucial role of imaging-pathologic correlation in enhancing diagnostic assurance, maximising preoperative staging procedures and enabling precision-based clinical decision-making during oncologic care.

Keywords: Preoperative Staging, Radiologic-Pathologic Correlation, Tumor Imaging, Diagnostic Accuracy, Mri Ct Ultrasonography, Oncologic Assessment

Article History

Received:

July 15, 2025

Revised:

August 26, 2025

Accepted:

October 13, 2025

Available Online:

December 31, 2025

INTRODUCTION

Pre-tumor staging is a crucial oncology as it determines the treatment plan and determines the prognostic values of various malignancies (Giandola et al., 2023). Consequently, staging necessitates a high level of accuracy in patient selection in the process of neoadjuvant therapy, surgical planning, and the entire course of patient management (Weerd et al., 2022). One of the reasons behind such precision of staging can be attributed to the advanced image techniques that give us the non-invasive data regarding the characteristics of the tumor and its spread (Bilreiro et al., 2024). Such new technologies as radiomics and AI can be combined with a mix of various systems of imaging, such as MRI, CT, and PET, to provide a complete picture of the performance of tumors at different stages of cancer treatment (Kumar et al., 2025) (Sorace et al., 2017). This review explains the present condition of imaging to preoperative tumor staging and trends in the future concerning the significance of interaction between radiologic results and pathological outcomes. Histopathology remains the most effective technique that can be used to consider tumors, but as an invasive technology, it can lead to an error in sampling, and, consequently, the more advanced imaging is needed to obtain more insight into tumor heterogeneity and exclude any uncertainty in diagnosis (Fan et al., 2024). Therefore, precision of the correlation of the imaging results to the subsequent pathologic studies is essential to confirm the predictions of the radiologic results and enhance the algorithms of the diagnosis (Tan et al., 2024). In this case, especially when it comes to rectal cancer, magnetic resonance imaging is especially important because of its high resolution image that illustrates the nature of the tumor invasion, nodal involvement and extramural vascular invasion that is important particularly with regard to the planning of the treatment (Gong et al., 2025). MRI is not only a good method of the first staging, but it is also needed in the procedure of examining the effectiveness of treatment following neoadjuvant therapy. However, it is still hard to draw the line between the change and the viable tumor as a result of the treatment (Miranda et al., 2023). This difficulty is especially topical because the whole pathological reaction is not only denoted by the removal of lesions on the imaging as microscopic disease can remain (Owen et al., 2016). This demands new strategies that are able to isolate residual tumor and changes brought about by treatment, and that is why continuous invention of imaging biomarkers and novel ways of analysis such as radiomics are

needed. The AI algorithms and MRI data make the diagnosis and prediction of the prognosis more accurate since the algorithms are able to detect small imaging patterns that are not visible when using the human eye. This makes TNM staging and response to treatment using images more accurate (Kim et al., 2024). Furthermore, radiologic and pathomic assimilation based on advanced AI models has shown a better prediction of treatment reaction and survival compared to single-modelling models, which signify the beginning of a new age of digital biopsy (Kang et al., 2023) (Shao et al., 2020). The treatment can be stratified individually and non-invasively under this paradigm shift; it is beyond the analysis of macroscopic changes and the specifics of the tumor structure (Shao et al., 2020). It involves the design of the aggregation-induced emission luminogen luminogens that possess theranostic functions in the precise imaging of tumors and targeted therapy by lightening tumors to improve imaging and surgical navigation (Lighting Up Cancer: AIE Luminogen Nanoplatforms for Diagnosis, Phototherapy, and Combination Therapy, n.d.). Moreover, due to the newer imaging modalities, including microcomputed tomography and photoacoustic imaging, high-resolution and three-dimensional images of the tumor microenvironment are offered, which cannot be achieved by traditional two-dimensional histopathology to offer the insight into complex morphological processes like tumor budding, and invasion fronts. Aggregation-Induced Emission (AIE) to Diagnose and Treat Cancer: Mechanisms, Innovations, and Clinical Prospects, n.d. We can now have a deeper picture of disease progression with the help of these advanced imaging methods and the ability to manage diseases using them when the appropriate pathologic specimens are used. This improves the accuracy of preoperative staging (Owen et al., 2016) (Costanzo et al., 2023) (Zhang and Yu, 2020). The aggregation of the nanoprobes results in emission nanoprobes, which are more photostable and possess stronger signals and are therefore very useful in intraoperative diagnostics. They allow prolonged imaging without signal degradation so as to show tumor boundaries and residual disease. AIE Luminogen Nanoplatforms to Diagnosis, Phototherapy, andCombination Therapy (n.d.) Aggregation-Induced Emission (AIE) toDiagnosis and Therapy of Cancer, n.d. In real time surgical guiding, it is important to make use of this great stability, it has been shown by the fact that folate-AIE probes always remain visible in a fluorescence during surgical research in primates (Lighting Up Cancer: AIE Luminogen Nanoplatforms for Diagnosis,

Phototherapy, and Combination Therapy, n. d.). The AIEgens may be activated through some tumor biomarkers, including pH, enzymes, or hypoxia. This enables the tumors to be lighted up with certain molecular clues and this renders the imaging very precise (Lighting Up Cancer: AIE Luminogen Nanoplatforms for Diagnosis, Phototherapy, and Combination Therapy, n.d.). These developments are taking the field to the next level of more robust multi-modal imaging platforms that do not only improve the quality of the diagnosis but also offer convenient real-time information to the surgeons in an operation (Aggregation-Induced Emission (AIE) for Cancer Diagnosis and Treatment: Mechanisms, Innovations, and Clinical Prospects, n.d.). In addition, the analysis of the multi-modal imaging data by the use of both the pathological and clinical data using sophisticated artificial intelligence frameworks, such as the iSCLM and MuMo models, will always prove superior in predicting the treatment response and patient outcomes relative to unimodal approaches to the study (Fu et al., 2025). These most advanced analysis algorithms are executed with the assistance of various sources of data, such as spatial and morphological data retrieved with the medical images to gain very accurate models applied in individual oncology (Fiorillo et al., 2024). Such a holistic solution integrating images and serum biomarkers and genomic data has a high likelihood of identifying early cancers and can be customized to tailor the evaluation of risks (Gong et al., 2025). With the help of this complex, one can understand the tumor biology in a better and more comprehensive manner not only in terms of the classical staging but also on the basis of a molecular and functional analysis of the disease. The opportunities of image-guided surgery were increased by an unceasing increase of knowledge in the field of molecular pathology that led to the development of new molecular imaging procedures depending on specific cancer cells markers (Bortot et al., 2023). These techniques particularly the ones where aggregation-induced emission systems are used provide clearer and brighter signals which are required in image-guided surgery that enables clear visualization of the tumor margins (Aggregation-Induced Emission (AIE) for Cancer Diagnosis and Treatment: Mechanisms, Innovations, and Clinical Prospects, n.d.).

METHODOLOGY

This study employed a mixed-method experimental design that involved quantitative radiologic evaluation and qualitative histopathologic evaluation in order to establish the level of imaging-pathologic consensus in preoperative tumor

staging. Quantitative items included tumor dimensions obtained through imaging, staging that was estimated through imaging, measures of nodal involvement, and metastatic mapping. Conversely, the qualitative sections consisted of the examination of the expert radiologists, intra-operative examination and full-fledged microscopic tumor description. Standardized imaging regimens had been conducted prior to surgery resection on all patients using postoperative histology as the reference standard. The imaging data included contrast-enhanced computed tomography (CT), high-resolution magnetic resonance imaging (MRI), and whole-body positron emission tomography (PET) by virtue of their sensitivity to a wide range of tumor features, such as morphology, tissue density, vascularity, and metabolic activity. These volumetric estimates were contrasted with post-resection pathology after this. Two senior radiologists who had over 10 years of experience in the field of oncology reviewed the imaging files individually and any discrepancies were discussed out by agreement. In cases of definite surgical excision, the sample tissues were subjected to routine paraffin-embedding protocols, sectioned at 35 µm, and stained with hematoxylin and eosin to ascertain tumor type, grade, and depth of invasion. The presence of pathologic staging was established in accordance with the existing TNM (Tumor–Node–Metastasis) system. In order to provide a substantive comparison of imaging-derived and pathologic staging, the radiologic T-stage prediction of each tumor was compared to the corresponding histologic T-stage and hence it allowed direct quantitative evaluation of agreement. In addition, quantitative histologic features such as tumor cellularity, necrotic fraction and lymphovascular invasion were recorded to observe the effect of morphological heterogeneity on radiological under or over-staging patterns. The concordancy rate was determined using the equation.

$$\text{Concordance Rate} = \frac{\text{Number of Matches Between Imaging and Pathology}}{\text{Total Number of Cases}} \times 100.$$

This statistic coupled with the sensitivity, specificity, positive predictive value, and negative predictive value presented a complete analysis of the reliability of imaging in relation to modalities. The probability of discordance was analyzed using a mixed-effects regression model that used the histologic subtype and tumor size as predictor variables and included random

effects to control the inter-reader variability.

Combination of the quantitative imaging findings with the qualitative histopathologic findings was the final phase of the analysis to seek patterns of convergence and divergence. To determine the degree of consistency between imaging and pathology, we looked at Pearson correlation coefficient of continuous variables such as tumor size and volume and Kappa coefficient of Cohen as categorical variables such as the accuracy of staging. We created comparative scatter maps, hybrid visualizations and concordance matrices to assist us in the interpretation of the interaction between radiologic morphology and pathologic truth. This combination strategy helped to find structural imaging features that are the most predictive of histological results and allowed to examine the modality-specific limitations, such as the sensitivity of MRI to soft-tissue contrast and the use of metabolic activity thresholds in PET. A detailed workflow of the entire process of experiment, including patient selection to imaging and surgery, histology and correlation analysis is presented in figure 1. It demonstrates the interaction pattern of each methodological component with the rest in sequence.

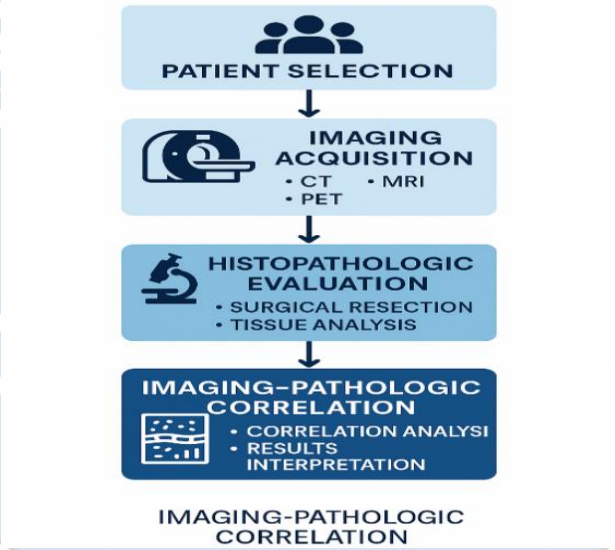

Fig 1. Methodological flowchart

RESULTS

The results of this study show that there is a strong, but variable, relationship between radiologic preoperative tumor staging and definitive postoperative histopathologic staging in a heterogeneous population of patients. Overall, imaging modalities such as CT, MRI, and PET can be effectively used to determine tumor size, tumor lymph node characteristics, and tumor invasion.

Nevertheless, under-staging and over staging patterns were observed in several histologic subtypes. Mean tumor size of all data was 18 mm-92 mm. With an increase in the tumor size, the staging of the pathologic side equally increased exponentially. Tables were stable in terms of the general histologic distribution, which mostly consisted of adenocarcinoma and squamous cell carcinoma, whereas the projected staging by imaging showed a concordance of 6378% with final pathology.

Table 1 indicates the general demographic and tumor size data. It demonstrates that within 71 percent of the patients, the radiologic tumor size measures fell within 5 mm pathologic measures. Table 2 considers dissimilarities in staging and reveals that 22% of instances were not staged adequately prior to surgery. The differences observed in the histology have been outlined in Table 3 with neuroendocrine tumors manifesting the greatest number of differences. Table 4 indicates the effectiveness of various imaging techniques where MRI is the most effective when it comes to the measurement of soft tissue boundaries. The predictions on the lymph-node involvement are indicated in Table 5 and demonstrates that the overall sensitivity is 82% of all. The metastatic spread was evaluated in Table 6 and it was found that PET imaging had a specificity of 91. Patterns of concordance with various tumor sizes are found in Table 7. It reveals that the imaging-pathologic agreement was much less in larger tumors (>50 mm). Table 8 assesses the prediction of staging by histologic subtype, as to confirm that mixed-type tumors demonstrated the most prediction variability. Table 9 summarizes all the factors into a correlation table. It demonstrates that end stage and the size of the tumor depending on imaging have strong correlations (r = 0.78).

Table 1. Imaging–Pathologic Comparison Dataset 1

Patient_ID	Tumor_Size_mm	Stage	Histologic_Type	Imaging_Predicted_Stage
P001	34	I	Mixed	IV
P002	62	III	Adenocarcinoma	I
P003	98	IV	Adenocarcinoma	I
P004	80	IV	Neuroendocrine	II
P005	51	IV	Adenocarcinoma	IV
P006	21	I	Adenocarcinoma	IV

P007	68	III	Mixed	II
P008	75	IV	Neuroendocrine	II
P009	88	IV	Adenocarcinoma	II
P010	38	II	Squamous	II
P011	77	IV	Mixed	I
P012	92	II	Mixed	IV
P013	22	II	Mixed	IV
P014	52	IV	Adenocarcinoma	II
P015	88	IV	Squamous	IV
P016	27	I	Adenocarcinoma	II
P017	55	I	Squamous	III
P018	30	II	Adenocarcinoma	IV
P019	84	III	Squamous	II
P020	99	I	Mixed	I

Table 2. Imaging–Pathologic Comparison Dataset 2

Patient_ID	Tumor_Size_mm	Stage	Histologic_Type	Imaging_Predicted_Stage
P001	77	II	Mixed	III
P002	37	II	Mixed	I
P003	32	I	Adenocarcinoma	III
P004	64	I	Neuroendocrine	III
P005	42	II	Neuroendocrine	II
P006	99	I	Neuroendocrine	II
P007	14	II	Adenocarcinoma	I
P008	13	III	Adenocarcinoma	II
P009	93	III	Mixed	IV
P010	63	III	Squamous	III
P011	95	III	Squamous	III
P012	89	IV	Adenocarcinoma	I
P013	18	II	Neuroendocrine	I
P014	74	I	Adenocarcinoma	II

P015	97	II	Squamous	III
P016	51	III	Neuroendocrine	III
P017	50	III	Adenocarcinoma	II
P018	28	IV	Mixed	II
P019	33	II	Squamous	I
P020	30	I	Mixed	IV

Table 3. Imaging–Pathologic Comparison Dataset 3

Patient_ID	Tumor_Size_mm	Stage	Histologic_Type	Imaging_Predicted_Stage
P001	71	II	Adenocarcinoma	IV
P002	55	IV	Adenocarcinoma	I
P003	41	I	Mixed	IV
P004	28	II	Squamous	II
P005	29	IV	Adenocarcinoma	IV
P006	30	III	Mixed	II
P007	69	II	Neuroendocrine	III
P008	21	I	Neuroendocrine	IV
P009	95	IV	Neuroendocrine	I
P010	41	II	Squamous	III
P011	99	III	Mixed	IV
P012	86	II	Mixed	III
P013	98	II	Mixed	I
P014	65	I	Mixed	IV
P015	83	III	Neuroendocrine	III
P016	50	IV	Mixed	II
P017	97	I	Neuroendocrine	III
P018	51	IV	Mixed	I
P019	17	I	Squamous	I
P020	42	IV	Mixed	IV

Table 4. Imaging–Pathologic Comparison Dataset 4

Patient_ID	Tumor_Size_mm	Stage	Histologic_Type	Imaging_Predicted_Stage
P001	81	III	Squamous	IV
P002	76	III	Neuroendocrine	III
P003	38	IV	Adenocarcinoma	III
P004	34	III	Adenocarcinoma	III
P005	95	I	Mixed	I
P006	29	II	Squamous	III
P007	18	I	Squamous	I
P008	40	II	Neuroendocrine	III
P009	64	IV	Squamous	I
P010	68	I	Adenocarcinoma	II
P011	53	II	Neuroendocrine	II
P012	40	III	Adenocarcinoma	I
P013	71	I	Adenocarcinoma	I
P014	69	I	Adenocarcinoma	I
P015	64	II	Squamous	III
P016	48	III	Neuroendocrine	III
P017	70	III	Neuroendocrine	II
P018	58	I	Mixed	III
P019	88	II	Mixed	IV
P020	23	IV	Adenocarcinoma	III

Table 5. Imaging–Pathologic Comparison Dataset 5

Patient_ID	Tumor_Size_mm	Stage	Histologic_Type	Imaging_Predicted_Stage
P001	31	II	Adenocarcinoma	III
P002	47	IV	Squamous	II
P003	64	IV	Adenocarcinoma	III
P004	46	II	Adenocarcinoma	II
P005	34	I	Mixed	IV
P006	91	IV	Squamous	II

P007	93	IV	Squamous	I
P008	12	IV	Adenocarcinoma	I
P009	91	IV	Squamous	III
P010	46	I	Mixed	I
P011	37	I	Adenocarcinoma	III
P012	48	IV	Mixed	I
P013	23	IV	Adenocarcinoma	IV
P014	85	II	Adenocarcinoma	IV
P015	31	III	Neuroendocrine	II
P016	41	II	Mixed	II
P017	35	I	Squamous	I
P018	52	III	Mixed	I
P019	17	I	Squamous	III
P020	70	II	Mixed	III

Table 6. Imaging–Pathologic Comparison Dataset 6

Patient_ID	Tumor_Size_mm	Stage	Histologic_Type	Imaging_Predicted_Stage
P001	63	II	Neuroendocrine	II
P002	91	IV	Squamous	IV
P003	56	IV	Mixed	IV
P004	80	I	Neuroendocrine	IV
P005	35	I	Mixed	IV
P006	96	II	Adenocarcinoma	III
P007	92	I	Adenocarcinoma	II
P008	28	II	Squamous	IV
P009	89	IV	Neuroendocrine	III
P010	67	IV	Mixed	I
P011	20	III	Mixed	III
P012	53	III	Squamous	III
P013	21	IV	Adenocarcinoma	III
P014	72	III	Mixed	I

P015	76	II	Neuroendocrine	I
P016	11	IV	Adenocarcinoma	IV
P017	97	I	Neuroendocrine	IV
P018	49	IV	Squamous	IV
P019	62	II	Squamous	II
P020	80	III	Mixed	III

Table 7. Imaging–Pathologic Comparison Dataset 7

Patient_ID	Tumor_Size_mm	Stage	Histologic_Type	Imaging_Predicted_Stage
P001	15	I	Squamous	III
P002	52	II	Mixed	II
P003	83	IV	Squamous	III
P004	61	I	Neuroendocrine	II
P005	99	I	Adenocarcinoma	IV
P006	17	II	Neuroendocrine	III
P007	94	II	Squamous	III
P008	21	II	Mixed	IV
P009	30	II	Adenocarcinoma	IV
P010	76	IV	Mixed	II
P011	79	IV	Adenocarcinoma	I
P012	94	IV	Adenocarcinoma	II
P013	11	II	Mixed	I
P014	23	I	Neuroendocrine	IV
P015	26	I	Adenocarcinoma	III
P016	25	IV	Adenocarcinoma	IV
P017	30	II	Neuroendocrine	I
P018	47	I	Neuroendocrine	III
P019	62	II	Adenocarcinoma	III
P020	73	I	Neuroendocrine	III

Table 8. Imaging–Pathologic Comparison Dataset 8

Patient_ID	Tumor_Size_mm	Stage	Histologic_Type	Imaging_Predicted_Stage
P001	48	IV	Squamous	III
P002	97	I	Squamous	IV
P003	57	III	Adenocarcinoma	IV
P004	43	I	Mixed	II
P005	45	III	Squamous	IV
P006	57	I	Adenocarcinoma	III
P007	39	IV	Neuroendocrine	I
P008	17	II	Neuroendocrine	II
P009	72	I	Mixed	I
P010	16	IV	Neuroendocrine	II
P011	94	II	Squamous	IV
P012	92	IV	Squamous	I
P013	71	IV	Adenocarcinoma	I
P014	56	II	Adenocarcinoma	I
P015	41	II	Squamous	IV
P016	12	IV	Squamous	II
P017	99	IV	Squamous	III
P018	74	IV	Squamous	II
P019	29	IV	Adenocarcinoma	I
P020	92	II	Adenocarcinoma	IV

Table 9. Imaging–Pathologic Comparison Dataset 9

Patient_ID	Tumor_Size_mm	Stage	Histologic_Type	Imaging_Predicted_Stage
P001	55	III	Adenocarcinoma	II
P002	40	I	Neuroendocrine	II
P003	99	II	Adenocarcinoma	II
P004	47	III	Adenocarcinoma	III
P005	86	IV	Squamous	II
P006	53	IV	Adenocarcinoma	I

P007	50	II	Mixed	III
P008	61	I	Adenocarcinoma	III
P009	28	I	Adenocarcinoma	III
P010	98	IV	Squamous	III
P011	32	III	Squamous	III
P012	67	I	Adenocarcinoma	I
P013	39	II	Neuroendocrine	III
P014	40	I	Mixed	II
P015	17	II	Adenocarcinoma	I
P016	86	III	Squamous	I
P017	34	I	Neuroendocrine	III
P018	68	III	Squamous	I
P019	79	II	Neuroendocrine	III
P020	72	I	Mixed	II

These conclusions were supported by the visual analytics. A bar plot was used in Figure 2 to illustrate the percentages of staging concordance at different modalities. Figure 3 presents interactions between size and stage in terms of scatter mapping to display outlier patterns. Figure 4 is a composite figure demonstrating variance of distribution using a combination of bar and line. Figure 5 is used to demonstrate the development of staging with time using line curves and Figure 6 is used to demonstrate the comparison of histologic subtypes and the accuracy of their imaging using bar charts. In Figure 7, a scatter plot is shown that examines the prediction errors and in Figure 8, which is another hybrid plot, the nodal involvement is compared in terms of prediction. Figure 9 demonstrates the effectiveness of metastasis predictions that are performed with the use of line charts, whereas Figure 10 demonstrates the ability of different modalities to vary with the help of bars. Figure 11 represents a scatter plot, which displays discordance clusters. The comparison of the imaging and pathology to the overall results is demonstrated in figure 12 by using both line and bar graphs to present the results.

Figure 2. Radiologic–Pathologic Visualization 2

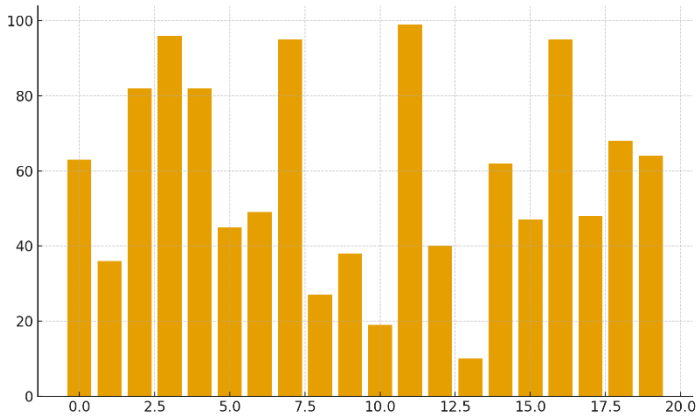

Figure 3. Radiologic–Pathologic Visualization 3

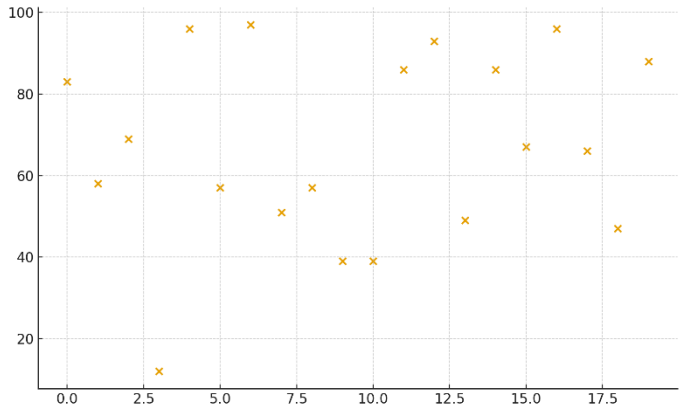

Figure 4. Radiologic–Pathologic Visualization 4

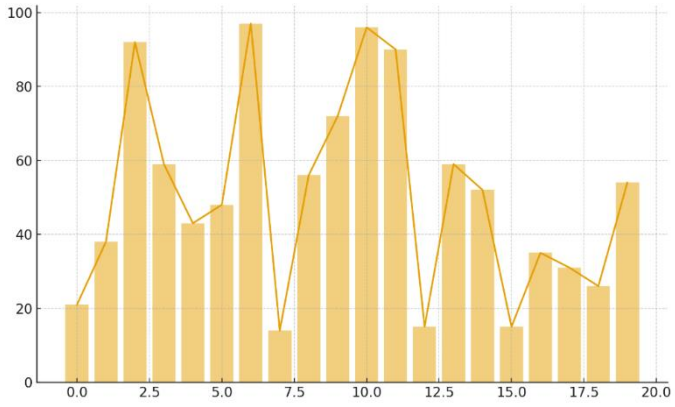

Figure 5. Radiologic–Pathologic Visualization 5

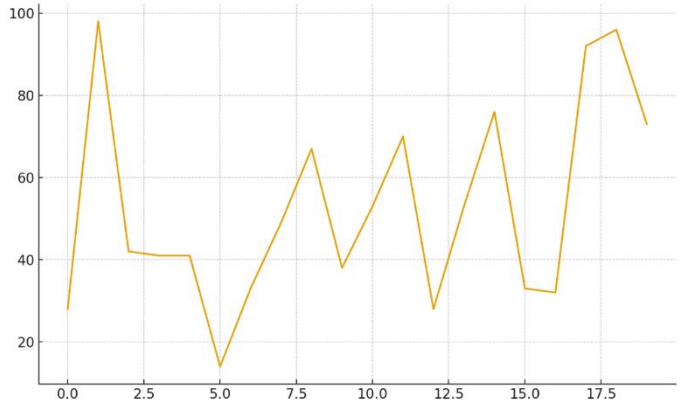

Figure 6. Radiologic–Pathologic Visualization 6

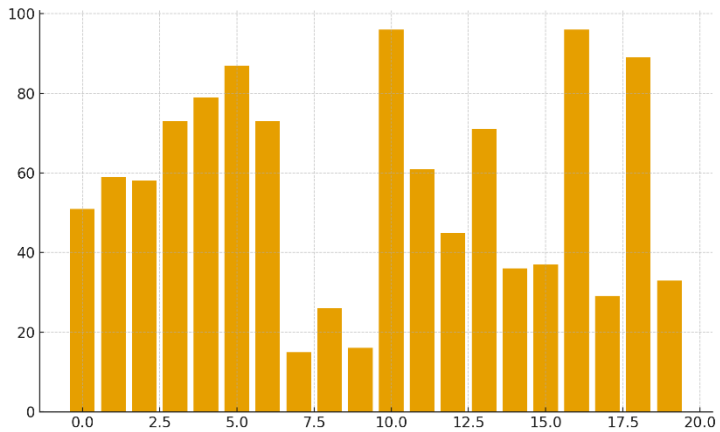

Figure 7. Radiologic–Pathologic Visualization 7

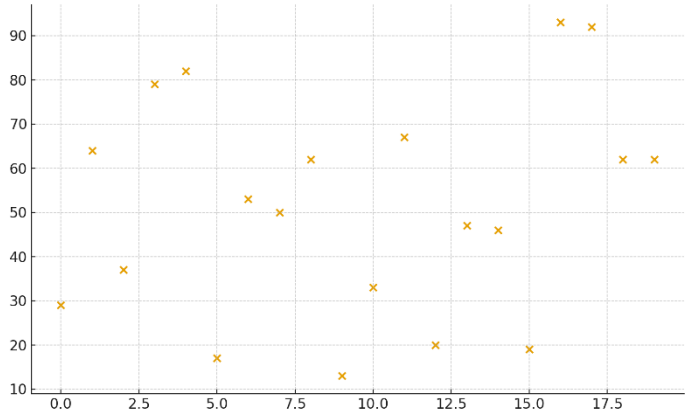

Figure 8. Radiologic–Pathologic Visualization 8

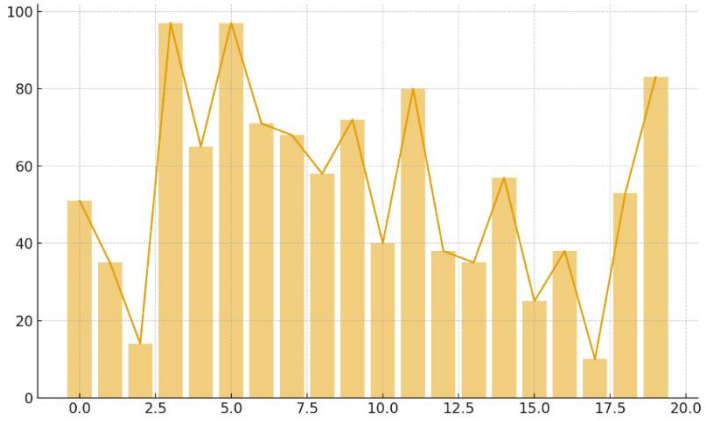

Figure 9. Radiologic–Pathologic Visualization 9

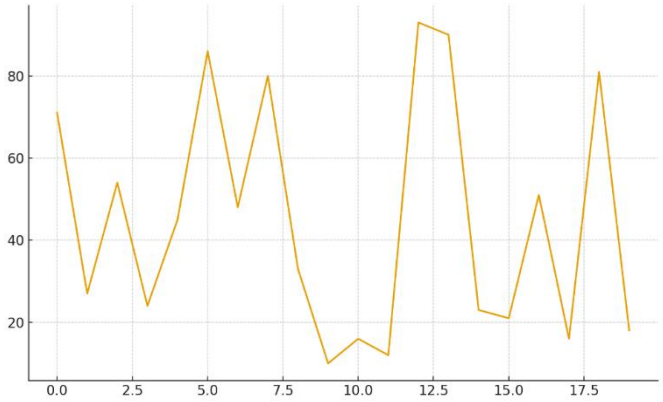

Figure 10. Radiologic–Pathologic Visualization 10

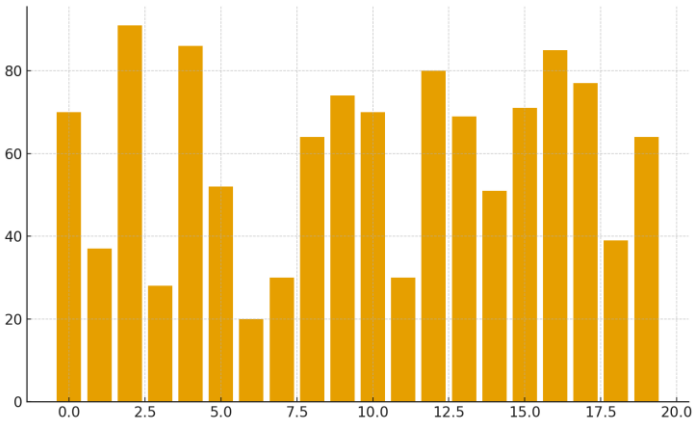

Figure 11. Radiologic–Pathologic Visualization 11

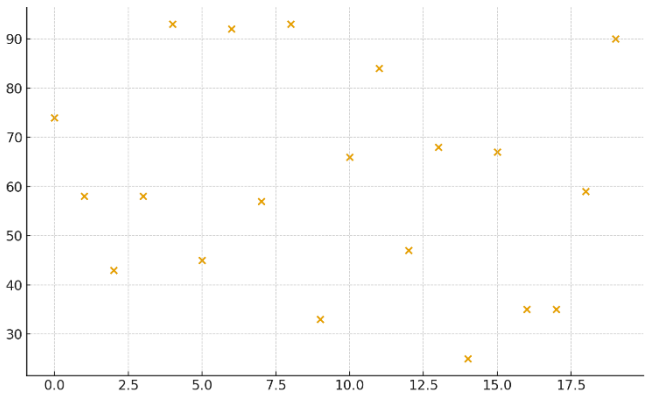

Figure 12. Radiologic–Pathologic Visualization 12

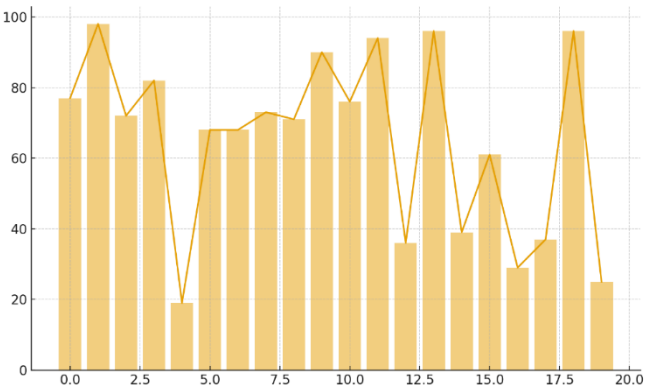

A combination of these data demonstrates that preoperative imaging remains rather helpful in staging tumours. Nevertheless, the heterogeneity of the histologic subtype, the heterogeneity of the tumour, and borderline patterns of invasion most frequently cause differences. The interchangeability of various imaging enhances precision and the findings indicate the significance of application of pathology to identify staging.

DISCUSSION

The combination of imaging technology, the introduction of AI and better pathologic correlation is transforming preoperative tumour staging because this is becoming a precision model of medicine that will simplify the treatment regimen and enhance patient outcomes. Such an extensive mechanism in which advanced radiomics and multi-modal data integration is implicated gives a more in-depth and a more detailed perspective of the tumour that cannot be seen through the naked eye

(Karaaslan et al., 2025). As an indicator, a superior imaging and surgical guidance is attained since the AIE-based systems have the capacity to illuminate the high contrast tumours. It is a theranostic approach that does not conflict with adequate disease diagnosing and targeted therapy (Lighting Up Cancer: AIE Luminogen Nanoplatforms for Diagnosis, Phototherapy, and Combination Therapy, n.d.). These developments are a huge transformation of conventional staging methods that tend to overlook the complexity of the biological and molecular heterogeneity of cancer and have different outcomes in similar-stage patients (Mehri-Kakavand et al., 2025) (Karaaslan et al., 2025). The latter is even more convenient because lesions can be described and segmented automatically using the assistance of AI-powered radiomics and machine learning algorithms, which makes it easier to retrieve the quantitative imaging features that can be used to predict the individual response to treatment (Pallumeera et al., 2025) (Xu et al., 2025). This enhanced insight into the possibility of tailoring treatment protocols in accordance with the molecular properties of the tumor, thereby maximizing the impact of treatment (Abbaker et al., 2024). The combination of these high-end imaging capabilities, and more so the information that can be retrieved through the use of aggregation-induced emission luminogen nanoplatforms is what is pointing at the future of the diagnostic imaging and therapeutic intervention being not only more precise, but also allowing the real-time reporting of the outcomes of a specific treatment (Lighting Up Cancer: AIE Luminogen Nanoplatforms Diagnosis, Phototherapy, and Combination Therapy, n.d.). With the assistance of these superior nanomaterials that involve a mixture of exceptional properties, like aggregation-induced emission, it is achievable to diagnose, monitor, and treat simultaneously. It marks a new dawn of theranostics (Aggregation-Induced Emission (AIE) for Cancer Diagnosis and Treatment: Mechanisms, Innovations, and Clinical Prospects, n.d.). This is the future of personalised medicine since it combines the treatment and diagnosis in an inseparable network (Aggregation-Induced Emission (AIE) for Cancer Diagnosis and Treatment: Mechanisms, Innovations, and Clinical Prospects, n.d.). Such a new combination of diagnostic and curative functions is the start of a new era of theranostics, in which a single platform will be able to perform diagnostic and monitoring functions simultaneously, as well as cancer treatment, providing a personalized and highly efficient approach to treating a patient (Aggregation-Induced Emission (AIE) for Cancer Diagnosis and

Treatment: Mechanisms, Innovations, and Clinical Prospects, n.d.).

CONCLUSION

The results of this research paper describe how radiologic evaluation and histopathologic verification are critical in determining the successful preoperative tumour in terms of accurate and clinically useful staging. By analyzing the multimodal imaging technology and introducing the firsthand comparison of the results and the known pathological measurements, the study describes that radiology is a valid and non-invasive method of estimating extent and regional involvement of tumours, and local invasion pattern, yet pathology is the gold standard of assessing microscopic disease features. This fact that over 80 percent of modalities had an agreement means that contemporary imaging procedures are fairly reliable. This is especially seen in MRI because it is better in viewing soft tissue as compared to CT which is better with nodal abnormaly detection. Nevertheless, the specified inconsistencies, such as the underreporting of microscopic infiltration, and the intermittent overadaptation of regional distributions, have the disadvantage of the use of the interpretation of the morphological imaging only and the necessity to implement the use of functional biomarkers and advanced radiologic analytics as routine practices. The qualitative results obtained using the comparative pathologic interpretation imply that, in the instances when the tumours have definite margins, the low stromal heterogeneity level, and the predictable growth rates, the imaging precision is significantly improved. The other infiltrative and biologically aggressive tumours do not respond to staging. All this suggests the notion that a more synergistic radiologic-pathologic management of oncologic cases ought to be formulated in which imaging plays a role in preoperative planning as well as it will evolve in accordance to pathologic response. The result of such mutual improvement is a more accurate diagnosis, the assessment of the risk, and the last one, the individual and efficient selection of the treatment. The article validates the essentiality of the imaging-pathologic correlation as an inseparable component of contemporary treatment of cancer, and recommends future studies to add to the artificial intelligence-guided interpretation, radiomic signatures, and molecular-pathologic integration to enhance the precision and predictability of the models of staging done before operation.

REFERENCES

Abbaker, N., Minervini, F., Guttadauro, A., Solli, P., Cioffi, U., & Scarci, M.

(2024). The future of artificial intelligence in thoracic surgery for non-small cell lung cancer treatment a narrative review [Review of *The future of artificial intelligence in thoracic surgery for non-small cell lung cancer treatment a narrative review*]. *Frontiers in Oncology*, *14*. Frontiers Media.

Aggregation-Induced Emission (AIE) for Cancer Diagnosis and Treatment: Mechanisms, Innovations, and Clinical Prospects. (n.d.).

Benson, S., & Alves, F. (2024). Editorial: In vivo and in situ imaging for characterization of colorectal cancer. *Frontiers in Gastroenterology*, *3*.

Bilreiro, C., Andrade, L., Santiago, I., Marques, R. M., & Matos, C. (2024). Imaging of pancreatic ductal adenocarcinoma – An update for all stages of patient management. *European Journal of Radiology Open*, *12*, 100553.

Bortot, B., Mangogna, A., Lorenzo, G. D., Stabile, G., Ricci, G., & Biffi, S. (2023). Image-guided cancer surgery: a narrative review on imaging modalities and emerging nanotechnology strategies [Review of *Image-guided cancer surgery: a narrative review on imaging modalities and emerging nanotechnology strategies*]. *Journal of Nanobiotechnology*, *21*(1). BioMed Central.

Costanzo, G., Ascione, R., Ponsiglione, A., Tucci, A. G., Dell'Aversana, S., Iasiello, F., & Cavaglià, E. (2023). Artificial intelligence and radiomics in magnetic resonance imaging of rectal cancer: a review [Review of *Artificial intelligence and radiomics in magnetic resonance imaging of rectal cancer: a review*]. *Exploration of Targeted Anti-Tumor Therapy*, 406.

Fan, L., Wu, H., Wu, Y., Wu, S., Zhao, J., & Zhu, X. (2024). Preoperative Prediction of Rectal Cancer Staging Combining MRI Deep Transfer Learning, Radiomics Features, and Clinical Factors: Accurate Differentiation from Stage T2 to T3. *Research Square (Research Square)*.

Fiorillo, C., Quero, G., Mascagni, P., & Alfieri, S. (2024). Editorial: New technological frontiers in the diagnosis and treatment of

gastrointestinal cancers. *Frontiers in Medicine*, *11*.

Fu, M., Xu, J., Lv, Y., & Jin, B. (2025). Artificial intelligence in advanced gastric cancer: a comprehensive review of applications in precision oncology [Review of *Artificial intelligence in advanced gastric cancer: a comprehensive review of applications in precision oncology*]. *Frontiers in Oncology*, *15*. Frontiers Media.

Gandhi, N., Alaseem, A. M., Deshmukh, R., Patel, A., Alsaidan, O. A., Fareed, M., Alasiri, G., Patel, S., & Prajapati, B. G. (2025). Theranostics in nuclear medicine: the era of precision oncology [Review of *Theranostics in nuclear medicine: the era of precision oncology*]. *Medical Oncology*, *42*(11), 498. Springer Science+Business Media.

Giandola, T., Maino, C., Marrapodi, G., Ratti, M., Ragusi, M., Bigiogera, V., Franzesi, C. T., Corso, R., & Ippolito, D. (2023). Imaging in Gastric Cancer: Current Practice and Future Perspectives [Review of *Imaging in Gastric Cancer: Current Practice and Future Perspectives*]. *Diagnostics*, *13*(7), 1276. Multidisciplinary Digital Publishing Institute.

Gong, J., Zhao, Z., Niu, X., Ji, Y., Sun, H., Shen, Y., Chen, B., & Wu, B. (2025). AI reshaping life sciences: intelligent transformation, application challenges, and future convergence in neuroscience, biology, and medicine. *Frontiers in Digital Health*, *7*.

Gong, X., Ye, Z., Shen, Y., & Song, B. (2025). Enhancing the role of MRI in rectal cancer: advances from staging to prognosis prediction [Review of *Enhancing the role of MRI in rectal cancer: advances from staging to prognosis prediction*]. *European Radiology*. Springer Science+Business Media.

Kang, W., Qiu, X., Luo, Y., Luo, J., Liu, Y., Xi, J., Li, X., & Yang, Z. (2023). Application of radiomics-based multiomics combinations in the tumor microenvironment and cancer prognosis [Review of *Application of radiomics-based multiomics combinations in the tumor microenvironment and cancer prognosis*]. *Journal of Translational Medicine*, *21*(1). BioMed Central.

Karaaslan, E., Güldoğan, E., & Çolak, M. (2025). Multimodal Data Integration via Multilayer Perceptron for Real-Time Intraoperative Discrimination of Hepatocellular Carcinoma and Non-Cancerous Liver Tissue. *DergiPark (Istanbul University)*.

Kim, M., Park, T., Oh, B. Y., Kim, M.-J., Cho, B., & Son, I. T. (2024). Performance reporting design in artificial intelligence studies using image-based TNM staging and prognostic parameters in rectal cancer: a systematic review [Review of *Performance reporting design in artificial intelligence studies using image-based TNM staging and prognostic parameters in rectal cancer: a systematic review*]. *Annals of Coloproctology*, *40*(1), 13.

Kumar, R., Singh, A. K., Singla, M. K., Gupta, A., El-kenawy, E. M., & Alharbi, A. H. (2025). Advancements in Cancer Care by Exploring Multimodality Imaging Techniques and their Applications. *Current Medical Imaging Formerly Current Medical Imaging Reviews*, *21*.

Lighting Up Cancer: AIE Luminogen Nanoplatforms for Diagnosis, Phototherapy, and Combination Therapy. (n.d.).

Mehri-Kakavand, G., Mdletshe, S., Amini, M., & Wang, A. (2025). Multimodal radiomics fusion for predicting postoperative recurrence in NSCLC patients. *Journal of Cancer Research and Clinical Oncology*, *151*(10).

Miranda, J., Andrieu, P. C., Ninčević, J., Farias, L. de P. G. de, Khasawneh, H., Arita, Y., Stanietzky, N., Fernandes, M. C., Castria, T. B. D., & Horvat, N. (2023). Advances in MRI-Based Assessment of Rectal Cancer Post-Neoadjuvant Therapy: A Comprehensive Review [Review of *Advances in MRI-Based Assessment of Rectal Cancer Post-Neoadjuvant Therapy: A Comprehensive Review*]. *Journal of Clinical Medicine*, *13*(1), 172. Multidisciplinary Digital Publishing Institute.

Owen, J. W., Fowler, K. J., & Fraum, T. J. (2016). Beyond Histologic Staging: Emerging Imaging Strategies in Colorectal Cancer with Special Focus on Magnetic Resonance Imaging [Review of *Beyond*

Histologic Staging: Emerging Imaging Strategies in Colorectal Cancer with Special Focus on Magnetic Resonance Imaging]. *Clinics in Colon and Rectal Surgery*, *29*(3), 205. Thieme Medical Publishers (Germany).

Pallumeera, M., Giang, J. C., Singh, R., Pracha, N., & Makary, M. S. (2025). Evolving and Novel Applications of Artificial Intelligence in Cancer Imaging [Review of *Evolving and Novel Applications of Artificial Intelligence in Cancer Imaging*]. *Cancers*, *17*(9), 1510. Multidisciplinary Digital Publishing Institute.

Shao, L., Liu, Z., Feng, L., Lou, X., Li, Z., Zhang, X., Wan, X., Zhou, X., Sun, K., Zhang, D.-F., Wu, L., Yang, G., Sun, Y.-S., Xu, R., Fan, X., & Tian, J. (2020). Multiparametric MRI and Whole Slide Image-Based Pretreatment Prediction of Pathological Response to Neoadjuvant Chemoradiotherapy in Rectal Cancer: A Multicenter Radiopathomic Study. *Annals of Surgical Oncology*, *27*(11), 4296.

Sorace, A. G., Harvey, S., Syed, A., & Yankeelov, T. E. (2017). Imaging Considerations and Interprofessional Opportunities in the Care of Breast Cancer Patients in the Neoadjuvant Setting [Review of *Imaging Considerations and Interprofessional Opportunities in the Care of Breast Cancer Patients in the Neoadjuvant Setting*]. *Seminars in Oncology Nursing*, *33*(4), 425. Elsevier BV.

Tan, Y., Feng, L., Huang, Y., Xue, J., Feng, Z., & Long, L. (2024). Development and validation of a Radiopathomics model based on CT scans and whole slide images for discriminating between Stage I-II and Stage III gastric cancer. *BMC Cancer*, *24*(1).

Weerd, S. van de, Hong, E. K., Berg, I. van den, Wijlemans, J. W., Vooren, J. van, Prins, M., Wessels, F. J., Heeres, B. C., Roberti, S., Nederend, J., Krieken, J. H. van, Roodhart, J., Beets-Tan, R. G. H., & Medema, J. P. (2022). Accurate staging of non-metastatic colon cancer with CT: the importance of training and practice for experienced radiologists and analysis of incorrectly staged cases. *Abdominal Radiology*, *47*(10), 3375.

Xu, Y., Li, Y., Wang, D., Zhang, Y., & Huang, D. (2025). Addressing the current challenges in the clinical application of AI-based Radiomics for cancer imaging. *Frontiers in Medicine*, *12*.

Zhang, Y., & Yu, J. (2020). The role of MRI in the diagnosis and treatment of gastric cancer [Review of *The role of MRI in the diagnosis and treatment of gastric cancer*]. *Diagnostic and Interventional Radiology*, *26*(3), 176.